Int J Adv Manuf Technol (2018) 95:4671–4683
DOI 10.1007/s00170-016-9345-2

ORIGINAL ARTICLE

Establishing a theoretical model for abrasive removal depth of silicon wafer chemical mechanical polishing by integrating a polishing times analytical model and specific down force energy theory

Zone-Ching Lin[1] · **Ren-Yuan Wang**[2] · **Zih-Wun Jhang**[1]

Received: 9 April 2016 / Accepted: 15 August 2016 / Published online: 3 September 2016

Abstract This study uses the polishing pad with cross pattern, and it is supposed that the contact area between polishing pad surface of cross pattern and wafer is Gaussian distribution to establish and analyze an innovative abrasive removal depth theoretical model of chemical mechanical polishing (CMP) silicon wafer. In this model, it uses the binary image pixel division to calculate polishing times and it derives the contact force of each abrasive particle and uses the specific down force energy (SDFE) theoretical equation to calculate the abrasive removal depth on each abrasive particle after down force being applied. This study carries out CMP silicon wafer experiment as well as atomic force microscopy (AFM) measurement experiment of SDFE of silicon wafer. The abrasive removal depth of silicon wafer acquired from simulation analysis is compared with the abrasive removal depth of silicon wafer obtained from CMP experiment of silicon wafer, and the difference in between will also be analyzed. It shows that the difference between the results of simulation and experiment is in the acceptable range.

✉ Zone-Ching Lin
zclin@mail.ntust.edu.tw

Ren-Yuan Wang
yny@aaroc.edu.tw

Zih-Wun Jhang
M10203234@mail.ntust.edu.tw

[1] Department of Mechanical Engineering, National Taiwan University of Science and Technology, 43 Keelung Road, Section 4, Taipei, Taiwan

[2] Department of Mechanical Engineering, Army Academy R. O. C, 750 Longdong Rd., Zhongli City, Taoyuan County, Taiwan

Keywords Silicon wafer · Chemical mechanical polishing · Specific down force energy · Abrasive removal depth · Polishing times

1 Introduction

This study aimed at furthering technological development in the semiconductor industry. The current trends and technology regarding application of integrated circuits (ICs) involve polishing a silicon wafer substrate to ultra-thinness and then applying semiconductor processing technology on it. Therefore, this study examined and investigated the wafer abrasive removal depth theory of the chemical mechanical polishing (CMP) removal technologies of IC-miniaturized silicon wafers that involve polishing silicon wafers with cross-pattern polishing pad. This study combined the polishing pixel calculation model of binary image pixel division with the concept of specific down force energy (SDFE) to establish a theoretical model to determine silicon wafer abrasive removal depth. This study established a theoretical model of abrasive removal depth regarding silicon wafers polished by cross-pattern polishing pad. An analytical theoretical model on the abrasive removal depth of silicon wafer was conducted. Subsequently, CMP and atomic force microscopy (AFM) experiments were performed to verify the reasonability of the theoretical model of the silicon wafer abrasive removal depth. The results showed that the present study exhibited academic and technological originality. Besides, the simulation result of this study also shows the distribution of abrasive removal depth on the pixel positions of various sections of silicon wafer surface.

Invented by G. Bining in 1986 [1], AFM is a type of scanning probe microscopy. Previous scholars have investigated the measuring abilities and applications of AFM. Lüben and

Johannsmann [2] used the probe tip as a perfect sphere, applying a contact mode AFM to investigate probe deflection and vertical pressure on a quartz plate. Tseng [3] conducted an experiment by using AFM probes to scratch silicon wafers. The result showed that the depth and width of the scratched grooves increased as the number of scratch cycles and the down force of the probe increased. A regression analysis of the experiment data determined that the dimensions of nanogrooves scratched by the AFM probes exhibited a logarithmic form relationship with the down force of the probe and that the scratch cycles showed a power-law function relationship.

Preston [4] presented in 1927 the first CMP abrasion theoretical model, which was expressed as MRR = KPV, where MRR was material removal rate, P was pressure applied, V was relative speed of wafer to polishing pad, and K was Preston constant. As seen from the above equation, material removal rate is related to pressure applied and load. Later on, in 1990, Cook [5] further proposed the contact condition between abrasive particles and wafer surface and replaced the pressure and speed in Preston's equation by the positive stress and shear stress of the contact surface between abrasive particles and wafer, respectively. Cook also explored the wear effect produced from the contact between abrasive particles and wafer surface, as well as the chemical reaction happened. They were mainly applied to describe the CMP model for the polishing process of silicon dioxide material on wafer surface.

Employing the concept of contact mechanics, Chekina and Keer [6] analyzed the relationship between wafer surface morphology and contact pressure in the CMP wearing process under steady condition and explored that planarization effect related to geometric unevenness of surface and different surface materials.

Jiang et al. [7] suggested giving consideration to two-body wear model under the condition of rough surface contact and defined the wear energy of material. They supposed that the asperity peak of rough surface was conic, and the asperity distribution was Gaussian distribution. Lin [8] proposed an analytical model for the material removal rate during specimen polishing. His model was based on the micro-contact elastic mechanics, micro-contact elastic-plastic mechanics, and abrasive wear theory. He found that the equation of material removal rate from the specimen surface is the function of average diameter of slurry particles, pressure, the specimen/pad sliding velocity, Equivalent Young's modulus, root mean square (RMS) roughness of the pad, and volume concentration of the slurry particle. Besides, Jongwon [9] further discussed about the contact deformation effect model of abrasive particles and derived a volume removal model of individual abrasive particles. Lin and Chen [10] developed a calculation polishing times method by using binary image pixel division for chemical mechanical polishing.

Lin and Huang [11] observed changes of the amount of wafer substrate removed when a pattern-free polishing pad and hole-pattern polishing pad were used under different down forces, rotation speeds, abrasive particle sizes, and slurry volume concentrations. In addition, in accordance with regression analysis theory, a compensation parameter, C_{rv}, was developed regarding the error caused by a change in the volume concentration of the slurry.

Lin and Wang [12] present a theoretical model for abrasive removal depth for polishing sapphire wafer using chemical mechanical polishing with a polishing pad that has a cross pattern. Their model uses the binary image pixel division to calculate the pixel polishing times, an abrasive contact model for single pixel multiple abrasive particles, to estimate the contact force between single abrasive particle and wafer. After the contact force is calculated, it uses Hertz contact force theory to calculate the abrasive depth of a single abrasive particle on the surface of the silicon wafer. In their model, it is supposed that the contact area between polishing pad surface of cross pattern and wafer is flat. They did not consider the contact area between polishing pad surface of cross pattern and wafer that is Gaussian distribution, and they did not use the specific down force energy theoretical equation to calculate the abrasive removal depth of a single abrasive particle on the surface wafer.

The aforementioned references do not like this study that uses the cross-pattern polishing pad to polish silicon wafer and uses the binary image pixel division to calculate polishing times, the contact area between polishing pad surface of cross pattern and wafer surface that is Gaussian distribution, then derives the contact force of each abrasive particle and uses the specific down force energy theoretical equation to calculate the abrasive removal depth on each abrasive particle after down force being applied. Therefore, this study combines the polishing pixel calculation model of binary image pixel division with the concept of SDFE to establish a theoretical model of the abrasive removal depth.

2 Theoretical model and experimental method of SDFE

This study applied the SDFE theory to propose an innovative idea. First, the effect of the polishing slurry on the abrasive removal depth of a silicon wafer was excluded, and AFM was then applied to cut the unaffected silicon wafer. The SDFE value of a silicon wafer without polishing slurry was subsequently measured. The contact area between the surface of the polishing pad and wafer was assumed to exhibit a Gaussian distribution. Binary image pixel division was applied to induce a model of the required polishing times of the wafer. Subsequently, the combination of a theoretical and analytical model of polishing times with a calculation model for abrasive removal depth that

was based on the SDFE theory generated a theoretical model for the average abrasive removal depth of silicon wafers that did not consider the influence of polishing slurry.

In addition, through CMP experiment data, this study verified the average abrasive removal depth model regarding the reasonability of the simulation and the difference between model simulation and CMP experiment results.

2.1 Experimental apparatus and materials of AFM

Experiments were conducted using the Dimension 3100 atomic force microscope (Veeco, Digital Instruments) in the Nano Lab at Tungnan University, Taiwan. The AFM probe used in the experiment was a DT-NCHR diamond-coated probe. The thickness of the diamond coat was approximately 100 nm, and the semispherical tip of probe had a sphere radius of approximately 150 nm; thus, the diamond tip of probe was used as a semispherical cutting tool during the experiment. According to the manufacturer's instruction manual, the probe has a spring constant of 42 N/m and a resonance frequency of 320 kHz. To obtain a more accurate spring constant k_r, it used AFM in tapping mode to perform a frequency sweep to find the actual resonance frequency f_r of the probe. The natural frequency equation used in vibration mechanics, $f^2 = k/m$, indicates that the square of the probe resonance frequency is proportional to the spring constant of the probe cantilever. Thus, the spring constant of the probe can be expressed as $k_r = (f_r^2 \times k_v)/f_v^2$. The actual spring constant k_r of the experimental probe was calculated according to the resonance frequency f_v and spring constant k_v provided by the manufacturer and the measured actual resonance frequency f_r [13]. The measured actual frequency f_r was obtained by experiment, and the measured value of f_r was 385 kHz. Thus, $k_r = (f_r^2 \times k_v)/f_v^2 = 60.8$ N/m. The force-distance curve method was adopted to measure the applied down force of the probe on the cutted workpiece. The cantilever offset d of the probe under down force can be obtained from force-distance curve. The down force F_d can be obtained using the following equation [13]:

$$F_d = k_r d. \tag{1}$$

2.2 SDFE theoretical model and calculation method

SDFE is defined as being down force energy dividing the removed volume of down press of the workpiece by the AFM probe, and the down force energy can be obtained from the down force applied by the AFM probe multiplying the increased cutting depth. Thus, the equation of SDFE can be shown as Eq. (2): [13]

$$\text{SDFE(specific down force energy)} = \frac{F_d \times \Delta d_n}{\Delta V_n} \tag{2}$$

where F_d(μN) is the down force applied by the AFM probe on the workpiece, Δd_n (nm) is the increased cutting depth, and ΔV_n (nm^3) is the removed volume of down press on the workpiece. Since the removed volume of down press on the workpiece changes with an increase in the cutting depth Δd_n, ΔV_n is the function of the cutting depth Δd_n.

For the removal volume of the central region, the forward distance of radius of the spherical cap denotes the volume already removed. Thus, the removed volume during this time is 1/2 that of the spherical cap volume under a cutting depth. The equation of its removed volume is expressed as follows: [13]

$$V_1 = \frac{1}{2}\pi \times \Delta d_1{}^2 \left(R - \frac{\Delta d_1}{3}\right) \tag{3}$$

where R is the probe tip radius of the cutting tool, and Δd_1 is the cutting depth.

In the CMP process, the abrasive particles in the polishing slurry cut grooves on the wafers to a depth similar to the diameter of the abrasive particles grooves. The process was also similar to that of the aforementioned AFM probe cutting process of silicon wafers. SEM was applied to measure the diameter of the semispherical AFM probe. Subsequently, the aforementioned experiment of using AFM to cut silicon wafers that were unaffected by polishing slurry was applied. The down force was set first. After the cutting process, the cutting depth was measured. In accordance with Eq. (3), the removal volume was calculated. Subsequently, the SDFE value of silicon wafers that excluded the effect by the chemical reaction of polishing slurry was obtained.

3 Model and experiment of the abrasive removal depth of wafers polished through CMP with cross-pattern polishing pad

3.1 CMP experiment

This study applied a conventional CMP experiment that used SiO_2 abrasive particles to polish 2-in. silicon wafers. The machine used was the PM-5 polisher produced by the Logitech Company and was located in the Precision Manufacturing Laboratory of the National Taiwan University of Science and Technology. The polishing pads were RodelIC-1000 with a cross-groove pattern. The width of the cross grooves was 3 mm. The polishing slurry used was from the Sun Chion Company. The polishing slurry contained SiO_2 abrasive particles with a diameter of 50 nm and a volume concentration of 50 %. The rotational speed of the polishing pad and wafer carrier were both 60 rpm. The total down force of the CMP machine was 6 psi. The configuration of the cross-pattern polishing pad and wafer is shown in Fig. 1.

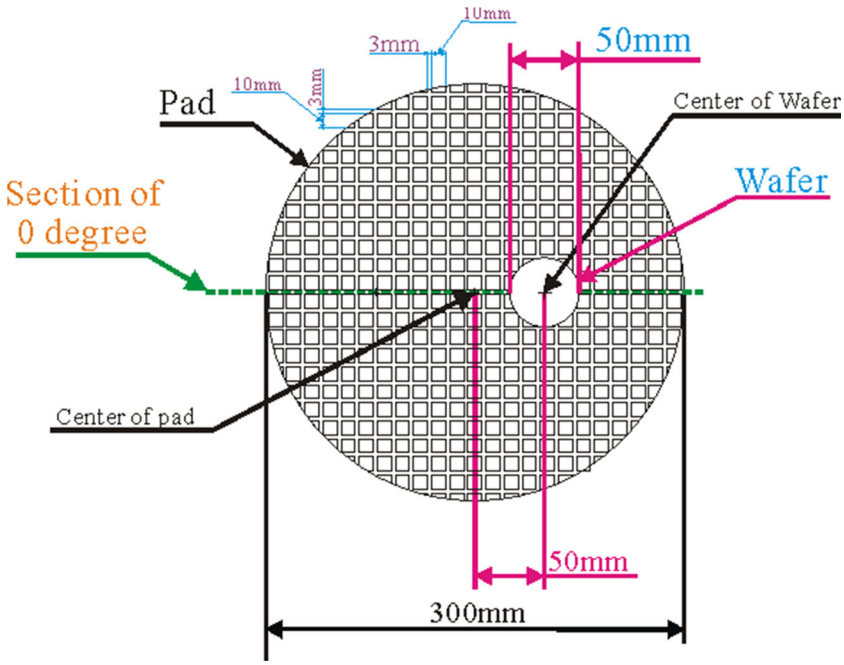

Fig. 1 Configuration of the cross-pattern polishing pad and wafer in conventional CMP

This study used precision electronic balance to measure the prepolishing wafer weight. Subtracting the postpolishing weight measured from the prepolishing weight obtained the abrasive removal weight in the experiment. Dividing the abrasive removal weight with the density of the silicon wafer obtained the abrasive removal volume. Subsequently, dividing the polishing removal volume with the silicon wafer area obtained the average abrasive removal depth. The average abrasive removal volume and average abrasive removal depth obtained from this CMP experiment could be further compared with the simulation results of the theoretical model of abrasive removal depth proposed in this study.

3.2 Model of wafer abrasive removal depth determined through CMP with cross-pattern polishing pad

The theoretical model in this study first applied the polishing times analytical model with unit time increment from the binary image pixel division method to calculate the contact times of the polishing pad and wafer pixels in unit time increment and to determine the effective contact pixels between the wafer and polishing pad. Subsequently, the per-pixel effective contact area between the roughness peaks of the polishing pad and the silicon wafer was calculated. This study then applied a polishing contact model of single pixel with multiple abrasive particles to calculate the contact force between a single particle and wafer per unit time increment. In accordance with the SDFE theory, the contact force was used to calculate the per-particle abrasive removal depth based on the SDFE value of the silicon wafer obtained from the AFM experiment. Subsequently, the per-pixel effective removal volume and average abrasive removal depth were calculated. Multiplying the polishing times per unit time increment with the average abrasive removal volume per pixel position obtained the average abrasive removal volume per unit time. Subsequently, dividing the average abrasive removal volume with the wafer area obtained the average abrasive removal depth.

3.2.1 Contact area between the roughness peaks of polishing pad and wafer

From a microcosmic perspective, the surfaces of all objects are rough. Therefore, when two surfaces contact each other, according to surface contact mechanics, two rough surfaces can be converted to one flat surface and one rough surface [14]. In analytical models of CMP volume removal, [14] other studies on removal rate have all followed this assumption, converting the surfaces of the wafer and polishing pad from two rough surfaces to a rough surface of the polishing pad and a smooth surface of the wafer. Consequently, pressure exerted on the surfaces was all undertaken by the contacting surface of the roughness peaks of the polishing pad.

This study used cross-pattern polishing pads and applied binary image pixel division to segment the polishing pad and wafer into individual pixels, as shown in Fig. 2. Figure 2 shows the illustration of the wafer and cross-pattern polishing pads as two 350 × 350 pixel value matrices; each pixel was 1 mm × 1 mm in size. In these matrices, the white pixels represent the surfaces of the polishing pad and wafer and are given a value of 1. By contrast, the black pixels represent the grooves of the polishing pad and are given a value of 0. Consequently, the grooves in the contact area between wafer

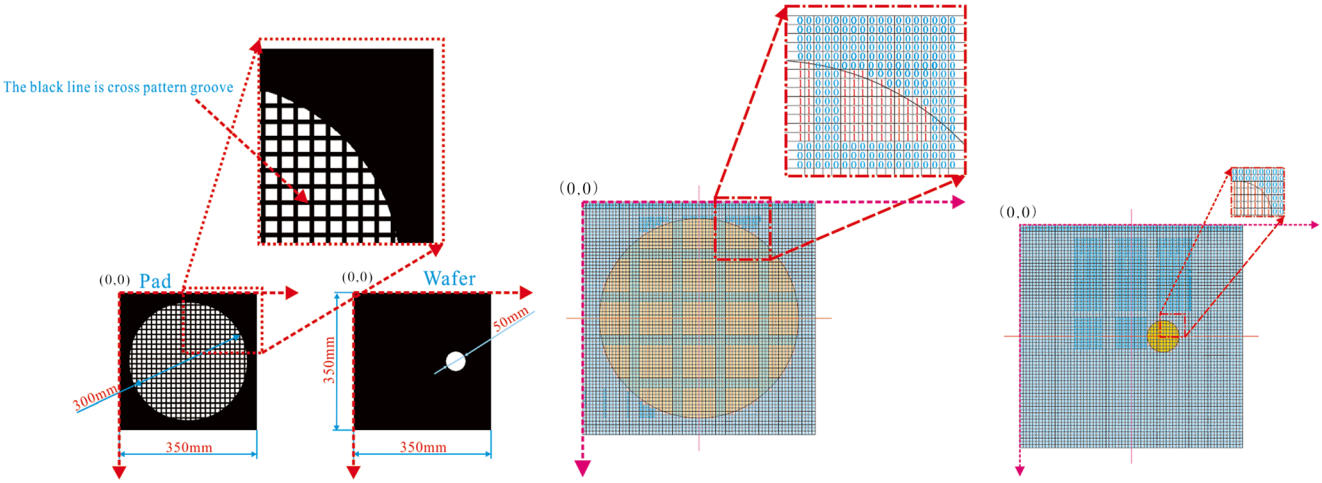

Fig. 2 Binary pixel matrices of the wafer and polishing pad

and polishing pad can be identified according to the value of these binary pixel value matrices.

Regarding the innovative concepts of applying cross-pattern polishing pads and binary image pixel division, this study referred to and revised the contact area and contact load equations in reference [15] to propose Eqs. (4) and (5), which are respectively used to calculate the per-pixel effective contact area (A_{rs}) and contact load (F) between the roughness peaks of the polishing pad and wafer. In addition, an assumption was made that only in the effective contact area (A_{rs}) between the roughness peaks of the polishing pad and wafer were abrasive particles embedded in the polishing pad. The silicon wafer was polished by these abrasive particles.

$$A_{rs} = \eta A_0 \pi \beta \int_h^\infty (z-h)\phi(z)dz \tag{4}$$

$$F(h) = \frac{4}{3}\eta A_0 E^* \beta^{\frac{1}{2}} \int_h^\infty (z-h)^{\frac{3}{2}}\phi(z)dz \tag{5}$$

$$\phi(z) = \frac{1}{\sigma\sqrt{2\pi}}\exp\left(-\frac{z^2}{2\times\sigma^2}\right) \tag{6}$$

where A_0 is the per-pixel contact area between the wafer and polishing pad, η is the area density of the roughness peaks in the polishing pad, h is the average gap between the pad and the wafer, and E^* is the equivalent Young's modulus.

$$E^* = \frac{1-\nu_p{}^2}{E_p} + \frac{1-\nu_w{}^2}{E_w} \tag{7}$$

where E_p is Young's modulus of the polishing pad, E_w is Young's modulus of the wafer, ν_p is Poisson's ratio of the polishing pad, and ν_w is Poisson's ratio of the wafer.

In this study, the related statistical parameter values of the roughness peaks of the polishing pad were determined in reference to those proposed in studies, as shown in Table 1.

From Eqs. (4) and (5), the following equation was obtained:

$$\frac{A_{rs}}{F} = \frac{3\pi\beta^{\frac{1}{2}}}{4E^*}\frac{\int_h^\infty (z-h)\phi(z)dz}{\int_h^\infty (z-h)^{\frac{3}{2}}\phi(z)dz} \tag{8}$$

The height distribution functional equation of the roughness peaks, Eq. (6), was substituted for Eq. (8). In accordance with [19], numerical integration was applied to Eq. (8), obtaining Eq. (9):

$$A_{rs} = C^{-1}\left(\frac{\beta}{\sigma}\right)^{\frac{1}{2}}\frac{F}{E^*} \tag{9}$$

where C is a constant.

According to [17], the constant C in Eq. (9) is calculated through deduction. In addition, [19] showed that the value of σ/h is generally between 0.5 and 3.0 and when σ/h is in the aforementioned range, the C value is approximately 0.35. The polishing pads used in this study were produced by the same company and were similar models as those used in [16]. Therefore, in Eq. (9), the values of variables β and σ were those used in [19]. The statistical parameter values are presented in Table 1. Because the pixel size used in this study was larger than the β and σ values, assessing the per-pixel valid contact area and contact load between the wafer and roughness peaks of the polishing pad was feasible. The variable E^* could be calculated by substituting values of related parameters in Table 1 into Eq. (7). Regarding F, it could be obtained in the following process: In a binary image pixel division model, the actual contact pixels between the silicon wafer and the roughness peaks of the polishing pad were first calculated. The contact force F value for per-pixel could then be obtained by dividing the total down force of the CMP machine with the effective contact pixels. Subsequently, this study used Eq. (9) to calculate the effective

Table 1 Statistical parameter values related to roughness peaks

Parameter	Explanation	Value
Ep [16]	Young's modulus of the polishing pad	100 MPa
σ [17]	The standard deviation of height distribution of the roughness peaks of the polishing pad	25 μm
β [17]	The average radius of the roughness peaks of the polishing pad	30 μm
v_p [16]	Poisson's ratio of the polishing pad	0.3
E_w [18]	Young's modulus of the silicon wafer	161.12 GPa
v_w [18]	Poisson's ratio of the silicon wafer	0.27
η [16]	The roughness peaks of the area density of the polishing pad	$2*10^8$ m^{-2}

contact area A_{rs} for per-pixel between the roughness peaks of the polishing pad and the wafer.

This study also involved assumptions as follows:

(1) The material removal of silicon wafer is mainly caused by the abrasive particles in the polishing slurry.
(2) The abrasive particles are only embedded in the A_{rs} of the polishing pads that contact wafers. Moreover, wafers are polished by these abrasive particles.
(3) The abrasive particles distribute uniformly.
(4) The abrasive particles are spherical and come in an average uniform size.
(5) The pressure exerted on the polishing pad is transferred to the wafer through the abrasive particles.
(6) The distance between contact points of neighboring abrasive particles is far enough that the interaction between neighboring contact points can be ignored.

On the basis of these assumptions, the number of contact pixels could be obtained through the analytical model of polishing times from the binary image pixel division method. The down force of each pixel of the wafer could be obtained by dividing the overall down force with the number of effective contact pixels. Adding the aforementioned to the number of effective abrasive particles in a single pixel position effective the down force of each abrasive particle (F_{aw}), according to SDFE theory, the abrasive removal depth of abrasive particles can be calculated from their down force.

3.2.2 Theoretical model of calculating average abrasive removal depth

This study takes the micro-contact mechanics of Greenwood and Williamson [20] as the foundation and supposes that the contact model between wafer and polishing pad is solid-to-solid contact. Hence, the analytic way of solid-to-solid contact is used to deduce and establish theoretical models. We also suppose that the removal of materials is mainly caused by the abrasive particles in slurry. Regarding this kind of removal model, the model of material removal volume (MRV) produced from the abrasive wear on the workpiece surface of polishing interface as indicated in the reference is expressed as equation [21]:

$$\mathrm{MRV}=n\bullet\mathrm{Vol} \tag{10}$$

n number of effective abrasive particles
Vol the removal volume of workpiece surface by a single abrasive particle

Dividing the material removal volume by time, the volume removal rate of polishing could be obtained.

This study presents a new CMP theoretical model of abrasive removal depth of silicon wafer polished by polishing pad with cross pattern. For this theoretical model, abrasive removal depth combines the theoretical model of the number of pixel polishing times of binary image dividing with the atomic force microscopy (AFM) measurement experiment of specific down force energy (SDFE) of silicon wafer. Under this model, the paper adopts the removal volume ($V_{\triangle t}$) of wafer at a single pixel position in a time increment (Δt), which can be expressed as:

$$V_{\triangle t}=N_e\bullet\mathrm{FF}(i',j')\bullet\mathrm{Vol} \tag{11}$$

N_e number of effective abrasive particles at each pixel position
FF(i',j') number of pixel polishing times of wafer by polishing pad at a single pixel position in a time increment
Vol material removal volume of the workpiece surface by a single abrasive particle

where FF(i',j') denotes the numerical value of the number of pixel polishing times calculated by time increment. The number of pixel polishing times is related to the relative speed of wafer to polishing pad. The relative speed of wafer to polishing pad (U_{CMP}) is expressed as Eq. (12):

$$U_{\mathrm{CMP}}=\sqrt{R_w{}^2\left(\omega_w-\omega_p\right)^2\cos\theta_w{}^2+D_{wp}{}^2\omega_w{}^2} \tag{12}$$

U_{CMP} relative speed of CMP wafer to polishing pad
$P(r_p,\theta_p)$ position of a certain point on the area of CMP polishing pad

(w_w, w_p) rotational speed of CMP wafer and polishing pad
D_{wp} distance between CMP wafer and the center of polishing pad

During this time, due to conversion of pixel length value to actual physical length value, the size of polishing frequency $F(i,j)$ should be multiplied by scale factor (SF) [10], as indicated in Eq. (13).

$$F(i,j) = \frac{U_{CMP}}{L} \times SF = \frac{\sqrt{R_w{}^2(\omega_w - \omega_p)^2 \cos\theta_w{}^2 + D_{wp}{}^2\omega_w{}^2}}{L} \times SF \quad (13)$$

U_{CMP} relative speed of CMP wafer to polishing pad
L length of pixel
$P(r_w, \theta_w)$ position of a certain point on the area of wafer
(w_w, w_p) rotational speed of wafer and polishing pad
D_{wp} distance between wafer and the center of polishing pad

As for scale factor (SF), since the size of pixel matrix to be captured depends on the need of accuracy, the pixel matrices in any different sizes can be captured. And each unit pixel represents an area unit with relative proportion. Between pixel length value and actual physical value, there is a certain proportion. Reference [10] regards this proportion as "scale factor" (SF), as shown in Eq. (14):

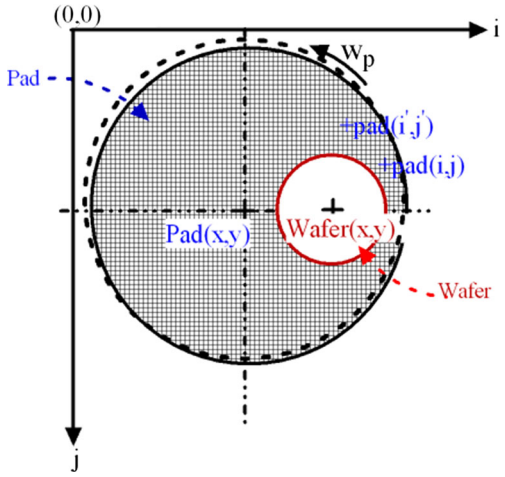

Fig. 3 The illustration of rotation positions between the wafer and polishing pad

$$SF = \frac{\text{diameter of the wafer profile of the design image}}{\text{pixel number on the wafer based on the diameter after converting wafer profile into image}} \quad (14)$$

After a unit of time, Δt, Fig. 3 shows the wafer and the polishing pad rotation, the polishing pad point (i,j) rotation to the point, (i',j'). The numerical value for the number of effective polishing times $FT(i',j')$ on the wafer surface is obtained by multiplying the polishing frequency $F(i,j)$ after rotation for a time increment, Δt, by the straight line-path effective polishing factor (SLEF(i',j')). The numerical value of the number of effective polishing times $FT(i',j')$ on the wafer is expressed as Eq. ((15)).

$$FF(i',j') = F(i,j) \times SLEF(i',j') \times \Delta t \quad (15)$$

Regarding the straight line-path effective polishing factor (SLEF), explanation has to be made here. The appearance of polishing pad and the design of pattern are not limited to the inside of wafer. Sometimes, in order to let the polishing of wafer edge remain effective, the appearance of polishing pad is usually designed to be larger than the pattern. During this time, after rotation for a unit of angle $\Delta\theta$, on the rotational path of polishing speed field may appear a phenomenon that the wafer is partially polished and partially not polished. In order to enhance the accuracy of analysis, and in consideration of the calculation characteristics of numerical value matrix, a modified model of "straight line-path effective polishing factor (SLEF)" [10] is proposed to make modification. The SLEF is expressed as Eq. (16):

$$SLEF = \frac{\text{total amount of the position value"1"on the polished wafer numcrical materix along the stright line−path}}{\text{total amount of the positions on the polished wafer numcrical matrix along the stright line−path}} \quad (16)$$

In addition, in Eq. (17), N_e is the number of effective abrasive particles at each pixel position. Suppose that the unit of volume concentration of the number of particles in slurry is χ, and the average diameter of abrasive particles is D_p , then

$\left(\frac{6\chi}{\pi D_p{}^3}\right)$ is the number of particles of a unit of volume in slurry. Therefore, the number of effective abrasive particles at a single pixel position is [16]:

$$N_e = A_{rs}\left(\frac{6\chi}{\pi D_p{}^3}\right)^{2/3} \tag{17}$$

Where χ is the unit of volume concentration of the number of particles in slurry is, D_p denotes the average diameter of abrasive particles, A_{rs} denotes the effective contact area of the polishing interface between polishing pad and wafer surface at a single pixel position. The effective contact area A_{rs} can be obtained from Eq. (9) which is determined from the contact area polishing pad surface of cross pattern and wafer is Gaussian distribution.

Since the size of each pixel is very tiny and the movement distance in a unit of time increment is 0.005 s, it is similar to a straight line in a unit of time increment. Thus, this study assumes that the removal volume of an abrasive particle polishes the wafer in a given time increment (Δt), as shown in Fig. 4 [22]:

$$\text{Vol} = A_p \bullet l \tag{18}$$

Vol the removal volume of an abrasive particle polishes the wafer in a given time increment
A_p cross-section area of the abrasive depth of an abrasive particle
l moved length of an abrasive particle in a given time increment

$$A_p \approx \frac{1}{2}\cdot\delta_{aw}\cdot 2r_a \approx \delta_{aw}\sqrt{\delta_{aw}D_p} \tag{19}$$

δ_{aw} the abrasive depth of a single abrasive particle on the wafer surface
r_a the average radius of the abrasive particles
D_p the average diameter of the abrasive particles

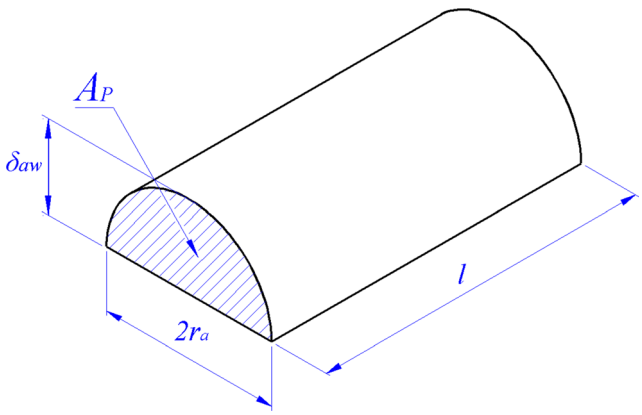

Fig. 4 Removal volume of a single abrasive particle in a time increment (Δt)

Therefore, the down force on each pixel of wafer is $F_{wp} = F_{total}/n$, where F_{total} denotes the total down force applied by polishing pad on wafer, and n denotes the number of effective contact pixels of wafer and polishing pad. Furthermore, the down force F_{aw} applied by a single abrasive particle on wafer can be obtained.

$$F_{aw} = \frac{F_{total}}{n \times N_e} \tag{20}$$

N_e denotes the number of effective abrasive particles of each pixel area. And the total down force F_{total} applied by polishing pad on wafer can be measured by CMP experimental machine. Through the above binary image pixel dividing method, the number of effective contact pixels n of wafer and polishing pad can be acquired. Besides, from the catalog provided by the manufacturer, the volume concentration (χ) of abrasive particles of slurry is known. Besides from Eq. (17), N_e can be obtained.

Therefore, F_{aw} can be obtained. Substituting the F_{aw} between a single abrasive particle and the wafer surface into the SDFE equation (Eq. 2) obtain the abrasive removal depth $\delta_{aw}(\Delta d_1)$ of a single abrasive particle on the wafer surface [13]:

$$\delta_{aw} = \Delta d = \frac{\Delta V \times \text{SDFE}}{F_{aw}} \tag{21}$$

Placing the result of Eq. (4) ($\Delta V_1 = \frac{1}{2}\pi \times \Delta d_1{}^2\left(R - \frac{\Delta d_1}{3}\right)$) into Eq. (21) and performing a further deduction obtains Δd which is the abrasive removal depth that a single abrasive particle causes on the wafer surface, as shown in Eq. (22):

$$\delta_{aw} = \Delta d = \frac{3R - \sqrt{9R^2 - \frac{24F_{aw}}{\pi \times \text{SDFE}}}}{2} \tag{22}$$

By placing Eq. (20) into Eq. (22), this study obtained the abrasive removal depth δ_{aw} a single abrasive particle causes to the surface of a wafer:

$$\delta_{aw} = \Delta d = \frac{3R - \left(9R^2 - \frac{24\times\frac{F_{total}}{n\times N_{e\,aw}}}{\pi\times\text{SDFE}}\right)^{\frac{1}{2}}}{2} \tag{23}$$

On the basis of the aforementioned deduction process, multiplying the wafer volume removed by a single abrasive particle in 1 unit of time with the number of effective abrasive particles obtains the effective removal volume in a single pixel position in 1 unit of time $V_{\Delta t}$. This study proposed that dividing $V_{\Delta t}$ with the wafer area of a single pixel position A_0 obtains the increment of average abrasive removal depth per single pixel position in 1 unit of time $\delta_{\Delta t}$:

$$\delta_{\Delta t} = \frac{V_{\Delta t}}{A_0} \tag{24}$$

Multiplying the effective removal volume in a single pixel position in 1 unit of time with the number of effective contact pixels between the wafer and polishing pad obtains the effective wafer removal volume in 1 unit of time. In addition, dividing the effective wafer removal volume in 1 unit of time with the wafer area obtains the average wafer abrasive removal depth in 1 unit of time.

4 Results and discussion

4.1 Polishing single crystal silicon with CMP experiment results

This study employed precision electronic balance to measure the prepolishing wafer weight. Subtracting the postpolishing weight from the prepolishing weight obtained the abrasive removal weight achieved through the experiment. Dividing the abrasive removal weight with the silicon wafer density obtained the abrasive removal volume. Subsequently, dividing the abrasive removal volume with silicon wafer area obtained the average abrasive removal depth. The CMP experiment in this study was conducted in the following conditions: the room temperature was 23 °C, the total down force was 6 psi, the rotational speed of the polishing pads and wafer was 60 rpm, the volume concentration of the polishing slurry was 50 %, and the diameter of abrasive particles was 50 nm. In total, 10 single crystal silicon specimens were polished for 10 min each. The experiment results revealed the removal weight, abrasive removal volume, abrasive removal depth, and abrasive removal depth per minute of each single crystal silicon specimen. Finally, the experiment results revealed that the average per-minute abrasive removal depth of the specimens was 105.8774 nm/min.

4.2 SDFE value experiment on silicon wafers unaffected by polishing slurry

An AFM experiment was conducted in this study to obtain the SDFE value of silicon wafers unaffected by polishing slurry. A probe with a spherical tip that had a radius of 150 nm was used. Several setpoint values were set in AFM machines, thus different down force values of 32.79, 38.5, and 47.31 μN were obtained. Cutting tools of AFM probe with different down force values were used to perform nanolinear cutting experiments on single crystal silicon substrates that were not dipped in polishing slurry. Table 2 shows the reactive of linear cutting v-shaped grooves in the first cutting pass under different down force values. With computer-aided design software, the volume removal volume amount of specific cutting depth could be calculated from the experimental results of down force and cutting depth in Table 2. Subsequently, SDFE Eq. (1) was applied to calculate the average SDFE value, which was approximately 0.01775 $\left({}^{\mu N\cdot nm}/_{nm}^{3}\right)$. Therefore, the SDFE value of silicon wafers unaffected by polishing slurry in this study was assumed to be 0.01775 $\left({}^{\mu N\cdot nm}/_{nm}^{3}\right)$.

4.3 Result analysis of the theoretical model of CMP abrasive removal depth of silicon wafers with cross-pattern polishing pads

All the equations of the theoretical model established in this study and employed to calculate abrasive removal depth were converted to computer programs by using MatLab. Cross-pattern polishing pad was applied as an analysis case and was illustrated as value matrices. In conditions similar to those applied in the experiment, namely a total down force of 6 psi, rotational speeds for both the polishing pad and wafer at 60 rpm, a volume concentration of the polishing slurry at 50 %, and the diameter of abrasive particles at 50 nm, the polishing times theoretical model of binary image pixel division was applied to polish the wafers for 1 min. The polishing times distribution on the wafer surface was obtained. Figure 5 displays a simulated distribution of polishing times of various pixel positions at the 45° line section on a silicon wafer surface.

The distribution of abrasive removal depth on silicon wafer surface is shown in Fig. 6, as determined on the basis of the analysis results of polishing times and by using the SDFE value of silicon wafer unaffected by polishing slurry and calculated according to AFM experiment, as well as by applying the value of abrasive removal depth in the theoretical model to simulate polishing wafer for 1 min. Figure 6 shows that the distribution trends of abrasive removal depth on all sections on the silicon wafer were similar. This was because the radial positions that centered on the wafer center exhibited a similar

Table 2 SDFE and relative data of linear cutting v-shaped grooves in the first cutting pass under different down force values

Experimental down force F_z (μN)	Cutting depth after the first cutting pass measured in the experiment $\Delta dz1$(nm)	Material removal volume calculated by the computer-aided design software (nm^3)	SDFE value calculated using theoretical Eq. (1) $\left({}^{\mu N\cdot nm}/_{E}^{3}\right)$	Average SDFE value of different down force experimental results $\left({}^{\mu N\cdot nm}/_{nm}^{3}\right)$
32.79	7.982	6299.14955	0.01775	0.017754
38.5	9.399	8703.37619	0.017756	
47.31	11.607	42,290.59343	0.017757	

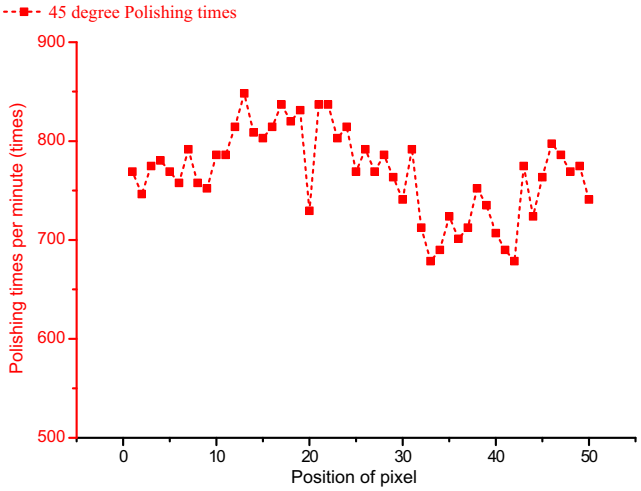

Fig. 5 Polishing times distribution at the 45° line section of the silicon wafer surface

relative velocity. In addition, Fig. 6 shows that areas that exhibited smaller abrasive removal depths were in line with the pixel positions corresponding to the grooves of the cross-pattern polishing pad. The distribution was similar to that of the polishing times, indicating that the grooves of the polishing pad had an influence. After 1 min of simulation polishing, the average per-minute abrasive removal depth was obtained as 94.7708 nm/min. This study assumed that the contact surface between the polishing pad and wafer exhibited a Gaussian distribution. According to the aforementioned A_{rs} equation, the actual per-pixel contact area A_{rs} was 0.3570 mm^2 in the first step simulation and the number of abrasive particles per pixel position was 138,463,935.

By applying binary image pixel division to segment the wafers and the cross-pattern polishing pad, this study determined the average abrasive removal depth of all pixel positions on the wafer. The average abrasive removal depth values

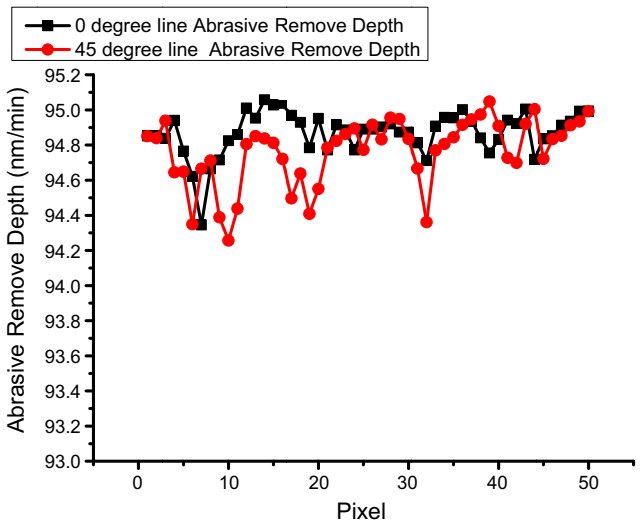

Fig. 6 Distribution of abrasive removal depth on the pixel positions of various sections of silicon wafer surface

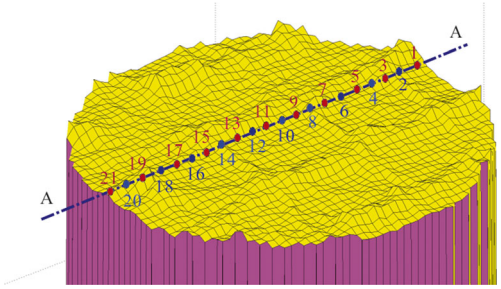

Fig. 7 Surface condition of the wafer after 1 min of simulation polishing

obtained after 1 min of polishing were converted to a 3D grid graph that illustrated the surface conditions of all the pixel positions on the silicon wafer surface, as shown in Fig. 7. Figure 7 reveals that the wafer surface pattern was similar to that of the polishing pad, indicating that the parts of the silicon wafer with relatively shallow abrasive removal depth (the relatively protruding parts in the figure) were caused by the grooves of cross-pattern polishing pads.

The CMP experimental results showed that the average abrasive removal depth per minute was approximately 105.8874 nm/min. However, the average abrasive removal depth per minute obtained through simulation was 94.7708 nm/min. The difference between the results obtained from the simulation and experiment was approximately 10.49 %. The main cause for this difference was that in the theoretical model, only the effect caused by the scratching of abrasive particles was considered, leaving several other variables unconsidered including the effect on abrasive removal depth caused by the chemical reaction initiated by the chemical composition of the polishing slurry and the influence of the display resolution of the binary pixel segmentation. Therefore, although the per-minute difference of abrasive removal depth between the theoretical simulation and experiment results was approximately 10.49 %, the theoretical model of abrasive removal depth that used CMP proposed in this study was deemed reasonable and acceptable, particularly when it applied cross-pattern polishing pads and did not consider the influence of a chemical reaction from the polishing slurry.

4.4 Measurement of wafer surface morphology

In order to obtain the morphological change of wafer surface cross-sections at different positions for the wafer having been polished 10 min by CMP under the down force of 6 psi as

Fig. 8 AFM-measured roughness (Ra) values at Position 1 and Position 2 on wafer surface for the wafer being polished 10 min under down force of 6 psi by CMP. **a** The measured roughness value (Ra) by AFM at Position 1 for the wafer being polished 10 min under down force of 6 psi by CMP. **b** The measured roughness value (Ra) by AFM at Position 2 for the wafer being polished 10 min under down force of 6 psi by CMP

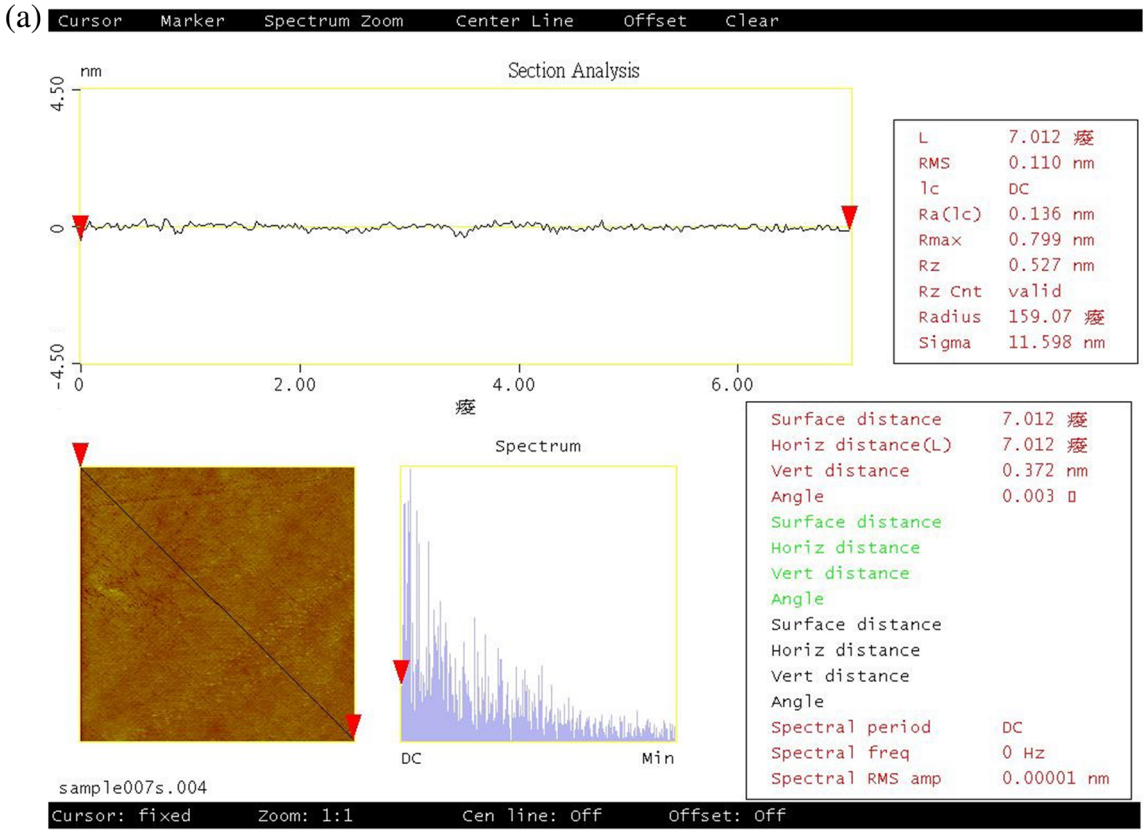

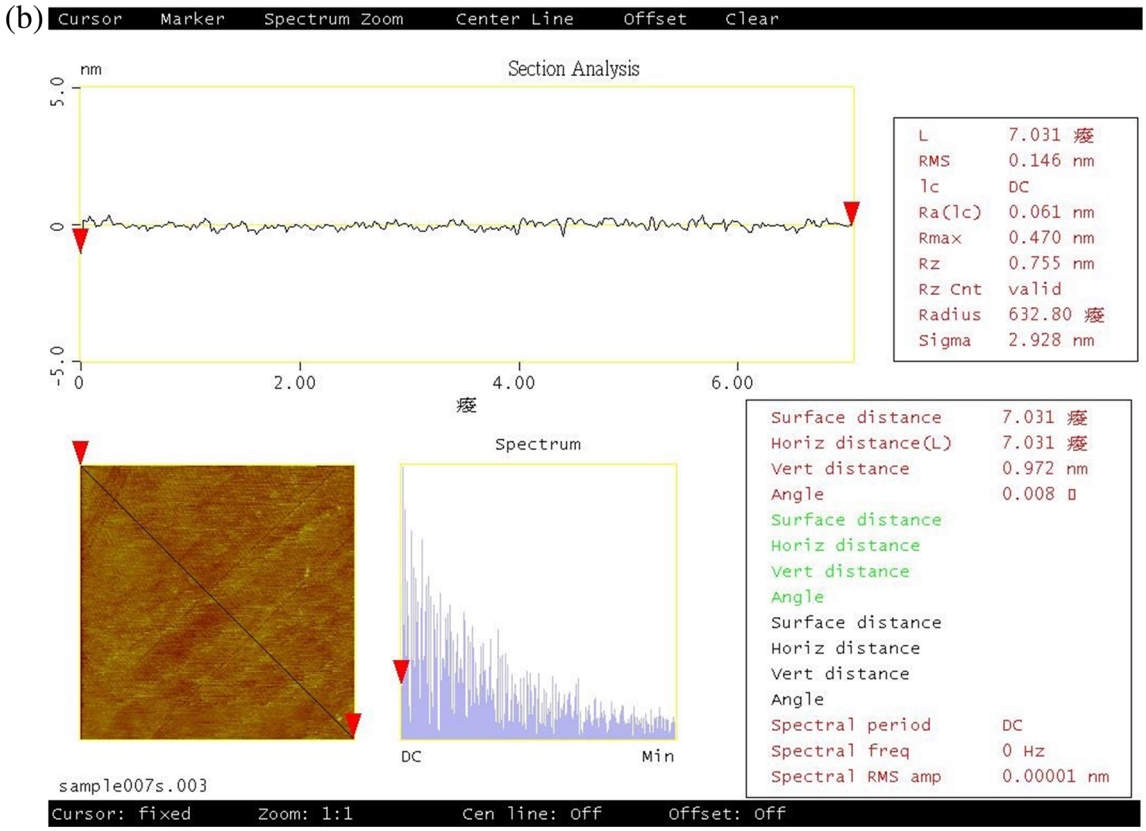

mentioned in CMP experiment, the paper uses AFM to select a contact mode that can obtain accurate surface morphology. The paper also conducts measurement of multiple points on wafer surface to acquire the average surface roughness values

at different points. The values of average surface roughness at different points can reflect the high or low morphology of wafer surface. After CMP experiment of wafer is completed, let the diameter direction of wafer surface go through the center of wafer, start taking positions of points at an interval of 2.5 mm from the two sides at a distance of 0.4 mm from the wafer edge and take the positions of total 21 points for measurement, with Point 1 to Point 21 as indicated on line A-A in Fig. 7. In Fig. 7, as mentioned above, it showed the 3D grid graph that illustrated the surface condition of all the pixel positions on the silicon wafer surface after simulating 1 min of polishing. Since the paper uses cross-pattern polishing pad to polish silicon wafer, as shown in Fig. 1, the groove width of cross pattern is 3 mm and let each distance of measured points be around 2.5 mm in order to ensure that the measured points can lie within the area affected by the pattern of polishing pad groove. The study uses AFM to measure the roughness values (Ra) of wafer surface for the wafer being polished 10 min under down force 6 psi at the 21 positions on measurement line A-A indicated in Fig. 7. For example, Fig. 8a shows the measured roughness value (Ra) by AFM is 0.063 nm at Position 1 in Fig. 7 for the wafer being polished 10 min under down force of 6 psi by CMP. Figure 8b shows the measured roughness value (Ra) by AFM is 0.186 nm at Position 2 in Fig. 7 for the wafer being polished 10 min under down force of 6 psi by CMP. The change of the measured roughness values by AFM at the 21 positions of line A-A of wafer surface for the wafer being polished 10 min under down force 6 psi by CMP is shown in Fig. 9, which could reveal the shape of cross-section of silicon wafer after polishing 10 min under down force 6 psi by CMP. Figure 9 shows the fluctuation of cross-section of average roughness values, and its trend appears to be the similar as the fluctuation of cross-section of line A-A in Fig. 7. Qualitatively speaking, it is also proven that the simulation result of the surface morphology trend of wafer appeared in Fig. 7 is reasonable. Besides, in Fig. 7, it indicates the simulation results of average abrasive removal depths obtained after 1 min of polishing are converted to a 3D grid graph that illustrates the surface conditions of all the pixel positions on the silicon wafer surface. And the curves results in Figs. 5 and 6 are also included in Fig. 7. Therefore, qualitatively speaking, it is also proven that the simulation result of curves in Figs. 5 and 6 are reasonable.

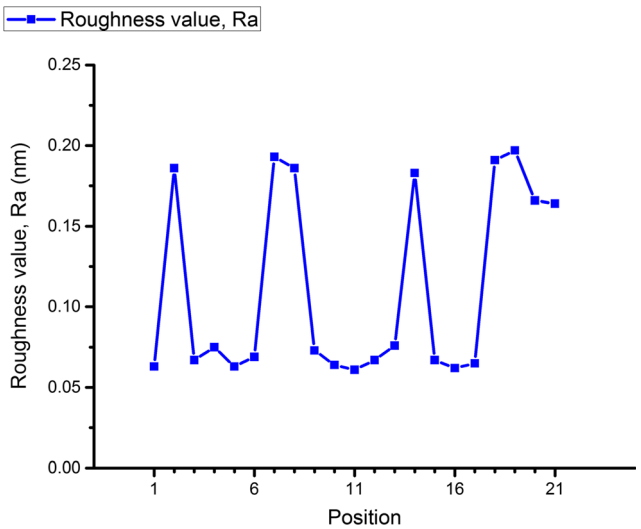

Fig. 9 The measured roughness value (Ra) by AFM at the 21 positions of line A-A of wafer surface for the wafer being polished 10 min under down force of 6 psi by CMP

5 Conclusion

This study first assumed that the contact area between the roughness peaks on the surface of the polishing pad with cross-patterned grooves and wafer surface had a Gaussian distribution. In addition, this study applied the SDFE theoretical equation that it established to calculate the abrasive removal depth of silicon wafers under the down force of an individual abrasive particle, without considering the chemical reaction of the polishing slurry. Subsequently, this study employed the theoretical model of polishing times that used binary image pixel division to develop an innovative theoretical model of silicon wafer abrasive removal depth that used CMP. A simulation analysis was also conducted. Through an AFM experiment, the single crystal silicon wafer SDFE value was obtained while ignoring the influence of the chemical reaction of the polishing slurry. Furthermore, comparing the abrasive removal depth of the silicon wafer obtained from the simulation analysis with that obtained from the CMP experiment revealed that the difference between the two results was approximately 10.49 %. The main cause for the difference in abrasive removal depth between the theoretical simulation and the experimental results was that the theoretical model established in this study only considered the effect caused by the scratching of abrasive particles, but ignored several other variables, including the effect on silicon wafers caused by the chemical reaction initiated by the chemical composition of the polishing slurry and the influence of the display resolution of the binary pixel segmentation. Therefore, the theoretical model of abrasive removal depth proposed in this study, which used CMP to polish silicon wafers while ignoring the chemical reaction of the polishing slurry, was determined reasonable. In addition, the surface condition of silicon wafers determined through the simulation showed that the surface pattern was affected by the cross pattern of the polishing pads. Specifically, the relatively shallow parts of the abrasive removal depth on the silicon wafers were caused by the grooves of the cross pattern on the polishing pads.

Acknowledgments The authors thank the Ministry of Science and Technology of Taiwan (grant number MOST 103-2221-E-011 -027) for supporting of this research.

References

1. Binning G, Quate CF, Gerber C (1986) Atomic force microscope. Phys Rev Lett 56:930–933
2. Lübben JF, Johannsmann D (2004) Nanoscale high-frequency contact mechanics using an AFM tip and a quartz crystal resonator. Langmuir 20:3698–3703
3. Tseng AA (2010) A comparison study of scratch and wear properties using atomic force microscopy. Appl Surf Sci 256:4246–4252
4. Preston FW (1927) The theory and design of plate glass polishing machines. J Soc Glass Technology 11:214–247
5. Cook LM (1990) Chemical process in glass polishing. J Non-Crystalline Solid 120:152–171
6. Chekina OG, Keer LM (1998) Wear-contact problems and modeling of chemical mechanical polishing. Journal of Electrochemical Society 145:2100–2106
7. Jiang J, Sheng F, Ren F (1998) Modeling of two-body abrasive wear under mutliple contact condition. Wear 217:35–45
8. Lin TR (2007) An analytical model of the material removal rate between elastic and elastic-plastic deformation for a polishing process. Int J Adv Manuf Technol 32:675–681
9. Jongwon S, Cyriaque PS, Kim AT, Tichy JA, Cale TS (2003) Multiscale material removal modeling of chemical mechanical polishing. Wear 254:307–320
10. Lin ZC, Chen CC (2005) Method for analyzing effective polishing frequency and times for chemical mechanical planarization polishing wafer with different polishing pad profiles. Journal of the Chinese Society of Mechanical Engineers 26:671–676
11. Lin ZC, Huang WS, Tsai JS (2012) A study of material removal amount of sapphire wafer in application chemical mechanical polishing with different polishing pads. Mechanical Science and Technology 26:2353–2364
12. Lin ZC, Wang RY (2014) Abrasive removal depth for polishing a sapphire wafer by a cross-patterned polishing pad with different abrasive particle sizes. Int J Adv Manuf Technol 74:25–38
13. Lin ZC, Hsu YC (2012) A calculating method for the fewest cutting passes on sapphire substrate at a certain depth using specific down force energy with an AFM probe. J Mater Process Technol 212: 2321–2331
14. Zhao Y, Maietta DM, Chang L (2000) An asperity microcontact model incorporating the transition from elastic deformation to fully plastic flow. J Tribol ASME 122:86–93
15. Qina K, Moudgilb B, Park CW (2004) A chemical mechanical polishing model incorporating both the chemical and mechanical effects. Thin Solid Films 446:277–286
16. Steigerwald JM, Murarka SP, Gutmann RJ (1997) Chemical mechanical planarization of microelectronic materials. John Wiley and Sons, New York
17. Yu T, Yu C, Orlowski M (1993) A statistical polishing pad model for chemical-mechanical polishing. Proceedings of the 1993 InternationalElectron Devices Meetings, IEEE, Washington DC, pp 865–868
18. El-Kareh B (1995) Fundamentals of semiconductor processing technologies. Kluwer Academic Publishers, Massachusetts
19. Johnson KL (1985) Contact mechanics. Cambridge University Press, Cambridge
20. Greenwood JA, Williamson JBP (1966) Contact of nominally flat surfaces. Proc R Soc London, Ser A 295:300–319
21. Luo J, Dornfeld DA (2001) Material removal mechanism in chemical mechanical polishing. IEEE Transaction on Semiconductor Manufacturing 14:112–133
22. Zhao Y, Chang L (2002) A micro-contact and wear model for chemical–mechanical polishing of silicon wafers. Wear 252:220–226